Evaluation of Electronic Coupling in a Donor-Bridge-Acceptor Molecule: A Fluorescence Polarization Anisotropy Investigation

Laura F. Cooley,*,† Hai Han,‡ and Matthew B. Zimmt*,‡

Physical Sciences Department, Rhode Island College, Providence, Rhode Island 02908 and Department of Chemistry, Brown University, Providence, Rhode Island 02912

Received: August 7, 2001; In Final Form: November 1, 2001

Electronic coupling magnitudes in donor−bridge−acceptor (DBA) molecules are influenced by the detailed structure of the bridge and its connections to the D and A groups. The influence of different symmetry, initial and final states on the electronic coupling magnitude, and on transfer dynamics has been investigated in single conformation ("rigid") DBA molecules with mirror plane symmetry elements. There is no uniformity of opinion on the magnitude of the "symmetry effect" in such systems. In this manuscript, the magnitude of the formally, symmetry forbidden electronic coupling between an excited anthracene donor, D*, and a cyclobutenediester acceptor across a three-bond bridge, DBA **1**, is determined through an analysis of the fluorescence polarization anisotropy of the charge transfer state to ground state ($CT \rightarrow S_0$) charge recombination emission. The wavelength dependence of the anthracene's absorption and emission band polarization are determined in a structurally related DBA molecule, **2**, that does not exhibit charge transfer absorption or emission bands. The polarization of these transitions agrees with the literature results for related anthracenes. Using the polarization data for the lowest energy anthracene absorption band ($S_0 \rightarrow S_1$), the polarization of the charge recombination emission in **1** is determined to be wavelength independent and to lie within the mirror plane symmetry element of the molecule (orthogonal to the anthracene short axis). These results demonstrate that the charge recombination emission derives negligible oscillator strength from the anthracene $S_1 \rightarrow S_0$ transition and that the electronic coupling between D* and A (i.e., between the S_1 and CT states) is too small to determine accurately by this method. The absorption polarization data from **1** provides evidence of a previously undetected, weak charge transfer absorption band ($S_0 \rightarrow CT$) on the red edge of the $S_0 \rightarrow S_1$ transition.

I. Introduction

Electron transfer events take place where attended by reasonable driving force and sufficient electronic interaction (coupling) between the donor (D) and acceptor (A) sites. In systems where the coupling is weak (nonadiabatic limit), the transfer rate constant is determined by the product of the reaction Franck−Condon factors and the square of the donor−acceptor electronic coupling matrix element, $|V|^2$.[1] As both factors influence the rate constant, it can be challenging to determine the magnitude of either quantity directly from experimental rate data. Accurate *relative* values of coupling magnitudes may be obtained from investigations in which the Franck−Condon factors are held relatively constant and the geometric parameters of the system are altered. Such experiments provide important data on the distance and orientation dependence of the electronic coupling.[2] The *actual* magnitude of the electronic coupling can be determined if the Franck−Condon factors are independently evaluated and/or varied.[3] In the latter case, the functional form for the dependence of the Franck−Condon factor on structural or environmental variables is usually assumed.

Although nonradiative electron transfer rate constants are strongly influenced by both Franck−Condon factors and electronic couplings, radiative electron transfer rate constants are determined by transition dipole moments.[4] Mulliken described a simple relationship between the transition dipole moment of a charge transfer (CT) transition and the electronic coupling matrix element between the initial and final diabatic states, $|V|$. In the following equation, $\Delta\mu$ is the difference of the system's dipole moment before and after electron transfer and ΔE is the vertical free energy difference between the two diabatic states involved in the radiative transfer event.[5]

$$M = |V|\,\Delta\mu/\Delta E \tag{1}$$

Mulliken's formalism provides a means to determine the electronic coupling, provided $\Delta\mu$ is known[6] and *only* the initial and final states determine the transition dipole moment (two-state model). Murrell recognized that the observed transition dipole moment could be increased by intensity borrowing from other electronic transitions within a molecule.[7] Mixing of the charge transfer state with higher lying donor or acceptor localized excited states (S_N) that have large transition dipole moments to the ground state (S_0) can increase the transition dipole moment between the CT and S_0 states. While the involvement of higher-lying states complicates determination of $|V|_{CT \leftrightarrow S_0}$ from radiative rate data, it does offer the possibility of evaluating $|V|_{CT \leftrightarrow SN}$ in cases where the intrinsic and borrowed transition dipole moment contributions can be separated. Verhoeven[8] and co-workers analyzed $CT \rightarrow S_0$ radiative rate constants to determine $S_1 \leftrightarrow CT$ electronic couplings in a family of thiacyclohexane and piperidine-derived donor−bridge−acceptor (DBA) molecules.[9] Gould[10] et al. analyzed the emission energy dependence of $CT \rightarrow S_0$ radiative rate constants (altered through variation of solvent polarity and donor oxidation potential) to

* Corresponding author.
† Rhode Island College.
‡ Brown University.

10.1021/jp013030c CCC: $22.00
Published on Web 01/16/2002

CHART 1

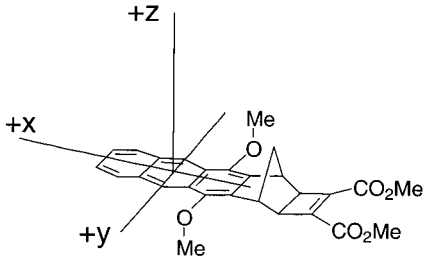

1

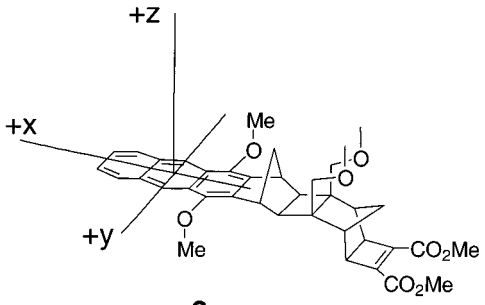

2

determine $|V|_{S_0 \leftrightarrow CT}$ and $|V|_{S_1 \leftrightarrow CT}$ in two families of exciplexes. Bixon[11] et al. determined $|V|_{S_1 \leftrightarrow CT}$ in a series of norbornane bridge derived DBA molecules by analyzing the solvent dependence of the charge recombination, radiative rate constants. Collectively, these studies demonstrate that donor−acceptor electronic coupling magnitudes can be determined via analyses of radiative transition dipole moments.

We sought to determine $|V|_{S_1 \leftrightarrow CT}$ in DBA molecule **1** (Chart 1), a short bridge (3-bond) member of a family of 1,4-dimethoxyanthracene donor, cyclobutenediester acceptor DBA molecules that were previously investigated with respect to the influence of molecular symmetry, bridge topology, and solvent on electronic coupling.[12] These molecules possess an approximate mirror plane symmetry element (symmetry group C_s) bisecting the donor, bridge, and acceptor. For DBA **1**, the ground state symmetry is A′, while the anthracene S_1 state, formed by promotion of an electron from the HOMO to the LUMO, has A″ symmetry.[13] The lowest energy singlet CT state, generated from the ground state by transfer of an electron from the anthracene HOMO to the cyclobutenediester LUMO, has A′ symmetry. Because the S_1 and CT state symmetries differ, nonradiative transfer of an electron between them is *formally* symmetry forbidden. Nonetheless, transfer occurs on a sub-nanosecond time scale in DBA **1**. Nonradiative, $S_1 \rightarrow$CT rate constants were analyzed for a 7-bond bridge member of this symmetry-forbidden family and for a 7-bond bridge member of a structurally similar, symmetry-allowed family.[12] It was found that $|V|_{S_1 \leftrightarrow CT}$ for the symmetry forbidden DBA was 10 to 15-fold smaller than for the symmetry allowed DBA. This translates into a 100- to 200-fold smaller value of the rate constant for the "forbidden" transfer at identical Franck−Condon factors. Bixon and co-workers analyzed CT radiative rate data in structurally related DBA molecules containing a dimethoxynaphthalene donor, a 3- or 4-bond bridge, and acceptors that established either symmetry allowed or forbidden $S_1 \leftrightarrow$CT interaction.[11] Their analysis presumed that symmetry forbidden $S_1 \leftrightarrow$CT couplings are insufficient to influence $S_0 \leftrightarrow$CT oscillator strengths but that symmetry-allowed $S_1 \leftrightarrow$CT interactions contribute to radiative recombination rates. By contrast, an investigation of symmetry effects on CT radiative rate constants in 7-bond bridge analogues of these allowed and forbidden topology molecules reported, at best, a small influence of state symmetry on the CT$\leftrightarrow S_0$ coupling.[14] Piotrowiak, Levy, and co-workers[15] investigated the dynamics of symmetry forbidden energy transfer between spiro-fused bichromophoric molecules in supersonic jets. They concluded that the "zero-order" picture overestimates the degree of symmetry control on electronic energy transfer and charge transfer rates. With different investigations providing contradictory conclusions regarding the influence of electronic symmetry on coupling, an alternative analysis of the $S_1 \leftrightarrow$CT coupling in **1** is warranted.

This manuscript reports steady state and time resolved fluorescence polarization anisotropy (FPA) investigations of the optical transitions in DBA molecule **1** and the 6-bond analogue **2** (Chart 1). The FPA dependence on excitation and emission wavelengths was determined for both molecules in viscous silicone oil at low temperatures. The FPA data from the $S_0 \rightarrow S_1$ transitions of **2** was used to establish the polarization of the dimethoxyanthracene absorption bands.[16] The fractions of long-axis (*x*-axis, Chart 1) and short-axis (*y*-axis, Chart 1) polarization of the absorption bands were determined as a function of excitation wavelength. This information was combined with the FPA data for **1**'s CT emission band to determine the fraction of *x*, *y*, and *z*-axis polarization of the CT$\rightarrow S_0$ transition. Since the direct, Mulliken type, $S_0 \leftrightarrow$CT transition dipole lies in the *x*−*z* plane (Chart 1), any *y*-polarization of the CT emission most likely arises from coupling (mixing) of the S_1 and CT states. The fraction of *y*-polarization in the CT emission along with the CT$\leftrightarrow S_0$ and $S_1 \leftrightarrow S_0$ transition dipole moments were used to establish an upper bound on the magnitude of the $|V|_{S_1 \leftrightarrow CT}$ electronic coupling. An estimate of $|V|_{S_3 \leftrightarrow CT}$ was derived by analyzing the relative magnitudes of the *x* and *z* polarizations of the CT$\leftrightarrow S_0$ transition dipole moment.

II. Experimental Section

A. Solvents and Sample Preparation. The viscous silicone oils used as solvents in this study were obtained from Gelest, Inc. and used without further purification. They are dimethylsiloxane polymers with trimethylsiloxy terminal groups. The two oils employed, Gelest DMS-T31 and DMS-T41, are referred to as G1000 and G10,000, respectively, where the numbers refer to the room-temperature viscosity in units of centistokes. Neither oil yielded significant fluorescence in this study. Samples were prepared by dissolving a very small amount of solid compound (<0.5 mg) in several drops of methylene chloride and adding a few mL of the silicone oil. Samples prepared in G1000 were stirred with a magnetic stirrer and then attached to a vacuum pump for at least thirty minutes to remove the methylene chloride. The high viscosity of G10,000 prevented use of a stirbar, so these samples were stirred manually then pumped for at least thirty minutes to remove the methylene chloride. Solutions were transferred to one cm path length, suprasil fluorescence cells, sealed, and stored in the dark for one to 5 h to allow bubbles formed during transfer to rise to the surface. Fluorescence cells were cooled to the desired temperature by immersion in an aluminum block with small openings for light entry and exit. The block was cooled using a 2-propanol solution circulated from a Neslab LT-50 bath. The temperature was monitored using a Cole-Parmer Digi-Sense thermocouple thermometer and a type T disk probe placed in direct contact with the wall of the fluorescence cuvette.

B. Steady-State Fluorescence Polarization Measurements. Steady-state fluorescence spectra were collected using a Spex F111XI fluorimeter system. Polarizers inserted into the excitation and emission paths within the sample compartment were aligned according to the following procedure provided by SPEX. A dilute solution (ca. 0.1%) of colloidal silica (Ludox, obtained from Aldrich) was employed as a scattering sample. The emission and excitation monochromators were set to 390 nm, and both polarizers were roughly aligned to transmit light polarized parallel to the lab vertical axis (VV setting). The excitation and emission slits were set to 1.3 mm (approximately 5 nm band-pass), and the excitation polarizer was rotated to achieve a rough maximum in the scattered light intensity, I_{VV}. The excitation polarizer was rotated 90°, to the approximate horizontal position (HV setting), and then adjusted to achieve a minimum signal. Each polarizer was then rotated 90° (VH setting), and the emission polarizer was adjusted to achieve a minimum in signal. This procedure was repeated until the polarization ratio, defined as $(I_{VV} \times I_{HH})/(I_{VH} \times I_{HV})$, was greater than 300 (corresponding to a measured anisotropy, $r >$ 0.99). The polarization ratio from dilute Ludox was periodically checked and found to be > 300 over the course of these experiments.

The steady state fluorescence anisotropy, r^{ss}, is defined as $r^{ss} = (I_{||} - I_{\perp})/(I_{||} + 2I_{\perp})$, where $I_{||}$ and $I_{\perp}$ refer, respectively, to the emission intensity polarized parallel and perpendicular to the excitation polarization. To correct for polarization sensitive transmission and diffraction characteristics in the detection monochromator and detector, standard correction factors[17] were applied:

$$r^{ss} = \frac{I_{VV} - GI_{VH}}{I_{VV} + 2GI_{VH}}$$

where $G = (I_{HV}/I_{HH})$. Steady state fluorescence spectra were obtained with the two polarizers in each of the four orientations (VV, VH, HV, and HH), and the anisotropy was calculated using the above equation.

Steady state fluorescence polarization measurements on solutions of **2** employed excitation slit widths of 0.5 mm and emission slit widths of 2.0 or 3.0 mm. The emission slit widths for the experiments with **1** were 3.0 mm. Increasing the excitation slits from 0.5 to 2 mm had no effect on the anisotropy results.

C. Time-Resolved Fluorescence Anisotropy Measurements. Time-resolved fluorescence decays were recorded using a home-built apparatus. The excitation pulse (388 nm, 40 ps, $< 1\ \mu J$) was vertically polarized (CVI CLPA10 polarizer: >100: 1) and passed through a Quantum Technology Inc. QK-10 Pockels cell for 300−400 nm. With no voltage, the Pockels cell was aligned to minimally depolarize the vertical excitation pulse (I_V:I_H > 80:1). The voltage needed to rotate the excitation pulse polarization to horizontal was determined. A home-built switching box, interfaced to the collection computer, toggled the voltage applied to the Pockels cell between zero (V polarization) and the predetermined voltage (H-polarization). Twenty fluorescence decays were averaged in four collection categories: vertical with excitation shutter closed, vertical with excitation shutter open, horizontal with excitation shutter closed, horizontal with excitation shutter open. The signals recorded with the excitation shutter closed were subtracted from the signals (with corresponding excitation polarization) recorded with the excitation shutter open to generate "background free" fluorescence decays. A small percentage of the excitation pulse was sampled prior to encountering the vertical polarizer and Pockels cell. The intensity of this light was used to normalize the vertical and horizontal "background free" fluorescence decays for variation in excitation light intensity. Five hundred to two thousand fluorescence decays were averaged and then scaled to produce the normalized vertical and horizontal fluorescence decay data.

III. Results

A. Reduced Absorption Spectra of the Anthracene Chromophore in 2. DBA **2** was used to determine the polarization of the dimethoxyanthracene absorption bands. The *x*, *y*, and *x*-axis polarized components of absorption spectra (reduced spectra) are most commonly determined using linear dichroism measurements.[18] Reduced absorption spectra may also be determined from wavelength-dependent excitation and emission anisotropies,[19] but this approach requires that the fractional *x*, *y*, and *z* polarizations are known at one or more wavelengths within the absorption or emission band.[19] The procedure employed in this analysis follows the work of Friedrich, Mathies, and Albrecht[19] who investigated the polarization of the absorption and emission transitions of anthracene. In the absence of molecular rotation, the fluorescence polarization anisotropy, $r(\lambda_{ex}, \lambda_M)$, exciting at wavelength λ_{ex} and detecting at wavelength λ_M, is given by[19]

$$r(\lambda_{ex}, \lambda_M) = \frac{3\Sigma - 1}{5} \qquad (2)$$

where $\Sigma = R_x(\lambda_{ex})Q_x(\lambda_M) + R_y(\lambda_{ex})Q_y(\lambda_M) + R_z(\lambda_{ex})Q_z(\lambda_M)$. In eq 2, R_ξ ($\xi = x, y, z$) are the fractions of the absorption coefficient polarized along the molecular *x*, *y*, and z-axes, respectively. The Q_ξ refer to the corresponding fractional components of the emission. At each wavelength the sum of the fractions must equal 1: $R_x(\lambda_{ex}) + R_y(\lambda_{ex}) + R_z(\lambda_{ex}) = 1$ and $Q_x(\lambda_M) + Q_y(\lambda_M) + Q_z(\lambda_M) = 1$. For the singlet−singlet transitions of the anthracene chromophore in the near UV and visible regions, the transition dipole moments are located in the plane of the ring (Chart 1). R_z and Q_z are insignificant and may be ignored without complication.[19,20] Accordingly, $R_x(\lambda_{ex}) = 1 - R_y(\lambda_{ex})$, $Q_x(\lambda_M) = 1 - Q_y(\lambda_M)$, and the fluorescence anisotropy is reduced to a function of $R_y(\lambda_{ex})$ and $Q_y(\lambda_M)$:

$$r(\lambda_{ex}, \lambda_M) = \frac{6R_yQ_y + 2 - 3(R_y + Q_y)}{5} \qquad (3)$$

The objective of this section is to determine $R_x(\lambda_{ex})$ and $R_y(\lambda_{ex})$ for the dimethoxyanthracene chromophore. Knowledge of the fractional, short-axis polarization, R_y, at a single excitation wavelength, λ_{ex0}, along with the experimentally determined emission anisotropy profile, $r(\lambda_{ex0}, \lambda)$ and eq 3 allow determination of the emission components, $Q_y(\lambda)$, at each wavelength within the anthracene emission. Subsequently, $R_y(\lambda)$ may be determined for the entire absorption spectrum from the experimental excitation anisotropy profile, $r(\lambda, \lambda_M)$, and $Q_y(\lambda_M)$. From a series of emission anisotropy profiles, $r(\lambda_{ex}, \lambda)$ at various λ_{ex}, and excitation anisotropy profiles, $r(\lambda, \lambda_M)$ at various λ_M, a self-consistent determination of $R_y(\lambda)$ and $Q_y(\lambda)$ may be effected, premised on an initial value of $R_y(\lambda_{ex0})$. This initial estimate of $R_y(\lambda_{ex0})$ was obtained from the reduced absorption spectra of anthracene[21] and a number of its alkyl[19] and dialkoxy[20] derivatives.

Figure 1 displays steady state, fluorescence excitation, and emission anisotropy profiles, r^{ss}, from the molecule **2** in G1000 silicone oil at −23 °C.[22] The anisotropy is largest for excitation *and* emission wavelengths of ∼400 nm and decreases as either

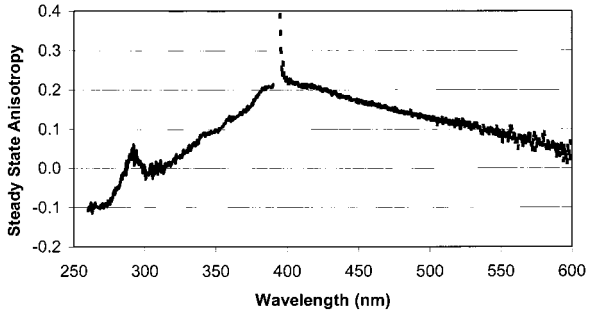

Figure 1. Steady state FPA from **2** in G1000 silicone oil at −23° C. Excitation anisotropy (left curve) detected at 410 nm. Emission anisotropy (right curve) excited at 388 nm. The steep spike in the emission profile near 400 nm is from scattered light.

the former is reduced or the latter is increased. Excitation at 268 nm, within the intense $S_0 \rightarrow S_3$ band, produces $r^{ss}(268, 400)$ equal to −0.11. Transitions within this absorption band are predominantly *x*-axis (long-axis) polarized in many anthracene derivatives, consistent with the negative value of the anisotropy.[19−21] For none of the excitation and emission wavelength combinations does the anisotropy attain values of 0.4 or −0.2, which would be expected for purely parallel or perpendicular absorption and emission transition dipole moments, respectively.[17] Rotation and libration of a chromophore during its excited state lifetime reduce the magnitude of the steady state anisotropy.[17] The effects of motion may be eliminated by temporally resolving the evolution of the anisotropy following excitation. Time resolved, polarized fluorescence decays were collected in G10000 silicone oil at −23 °C following excitation at 388 nm. The method of Christiansen[23] was used to determine the "motion free" value of the anisotropy, $r(\lambda_{ex}, \lambda_M)$. Polarized fluorescence decays were recorded at two wavelengths on the blue edge of the emission band and yielded motion-free values of $r(388, 405) = 0.34 \pm 0.02$ and $r(388, 420) = 0.31 \pm 0.01$. The corresponding values of r^{ss} (Figure 1) are 0.216 and 0.206. From these data, an average value of the ratio $r/r^{ss} = 1.54$ was obtained. Therefore, all steady-state emission and excitation anisotropy data from **2** were multiplied by 1.54 to generate the motion-free anisotropy, $r(\lambda_{ex}, \lambda_M)$.

The red edge of the first vibronic band in the absorption spectrum of 1,4-didecyloxyanthracene is purely *y*-axis (short-axis) polarized.[20,24] Thus, $R_y(410\text{ nm}) = 1.0$ was used as the initial estimate in the effort to determine $R_y(\lambda)$ and $Q_y(\lambda)$. This estimate, the motion-free anisotropy data, $r(410, 430-450)$, and eq 3 were used to evaluate $Q_y(430-450\text{ nm})$.[25] The resulting $Q_y(430-450\text{ nm})$ were combined with the experimentally determined $r(\underline{388}, 430-450)$ data and eq 3 to generate a value of $R_y(\underline{388}\text{ nm}) = 0.90 \pm 0.02$ (average of the results from 41 wavelengths). As the entire fluorescence spectrum is observable upon excitation at 388 nm,[25] $R_y(388\text{ nm})$ and the $r(388, 400-600)$ data were used to generate values of $Q_y(400-600\text{ nm})$. Average values of $R_y(260-410\text{ nm})$ were then determined from the Q_y at 410 nm (0.974), 439 nm (0.863), and 470 nm (0.803), and the corresponding $r(260-400, \lambda_M)$. Finally, a second set of average $Q_y(400-550)$ values were determined from the R_y at 320 nm (0.373), 350 nm (0.573), 370 nm (0.712), and 388 nm, and the corresponding $r(\lambda_{ex}, 400-550)$.

The bounds (0.0−1.0) on $R_y(\lambda)$ and $Q_y(\lambda)$ constrain the acceptable values of $R_y(388\text{ nm})$. In the iterative procedure described above, values of $R_y(388\text{ nm}) < 0.90$ generate $Q_y(400\text{ nm})$ that are larger than 1.02. Similarly, values of $R_y(388\text{ nm}) > 0.92$ produce $R_y(410\text{ nm}) > 1.03$ and $R_y(260\text{ nm}) < 0$. This constrains $R_y(388\text{ nm})$ to 0.91 ± 0.01, in good agreement with

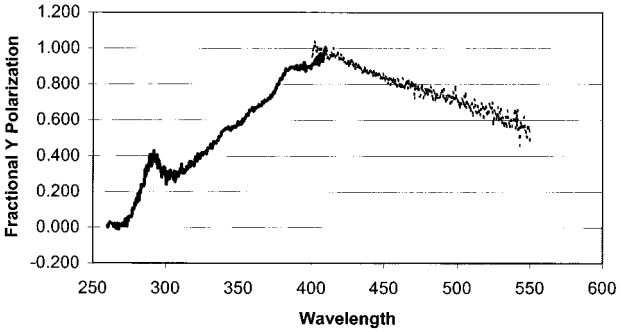

Figure 2. Fractional *y*-polarization of the $S_0 \rightarrow S_1$ (R_y, left curve) and $S_1 \rightarrow S_0$ (Q_y, right curve) transitions of **2**. Both curves are averages resulting from analyses of numerous excitation and emission anisotropy data sets (see text).

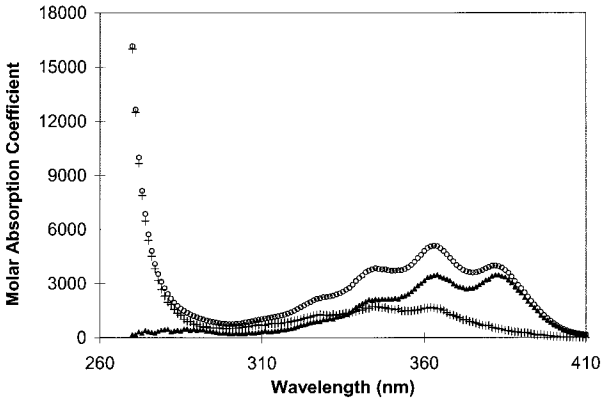

Figure 3. The molar absorption coefficient of the anthracene transitions in **2** (○) factored into its *y*-polarized (▲) and *x*-polarized (+) components (reduced spectra).

the value of 0.90 generated from the initial assumption that $R_y(410) = 1.0$. Figure 2 displays the final, self-consistent, $R_y(260-410\text{ nm})$ and $Q_y(400-550)$ resulting from a starting value of $R_y(388\text{ nm}) = 0.91$. The steady state, wavelength-dependent anisotropy curves predicted using the averaged R_y, Q_y and $r/r^{ss} = 1.54$ are in good agreement with the experimental results (Supporting Information, Figure S1). The *x*-polarized and *y*-polarized components of the absorption spectrum (reduced spectra) may be calculated as $(1 - R_y(\lambda)) \times \epsilon(\lambda)$ and $R_y(\lambda) \times \epsilon(\lambda)$, respectively (Figure 3). The first vibrational feature (383 nm) of the absorption is extensively *y*-axis polarized. The vibrational spacing in the *y*-polarized spectrum is ∼1360 cm^{-1}. The extinction coefficient at the vibronic peaks of the *y*-polarized spectrum decrease at shorter wavelengths, as does the modulation in this spectrum. The intensity of the *x*-polarized absorption spectrum increases from near zero at 410 nm to the first peak at 362 nm. Although there is very little modulation in the *x*-polarized spectrum, it appears that the first vibrational band of the *x*-axis polarized absorption is ∼1500 cm^{-1} to the blue of the first vibrational band in the y-polarized spectrum.[26] The vibrational spacing in the *x*-polarized spectrum is ∼1450 cm^{-1}. The intensity of the *x*-polarized absorption attains a maximum at 344 nm. The *x*-axis polarization of the intense absorption band in the 260−280 nm region is consistent with prior determinations in anthracene and derivatives.[19−21]

B. Polarization Components of the CT Emission from 1. Excitation (388 nm) of **1** at in G1000 silicon oil at −11 °C yields a steady state emission anisotropy plot (Figure 4) that is dramatically different from that of **2**. At wavelengths longer than 525 nm, the anisotropy is *wavelength independent* with the value -0.105 ± 0.010. At wavelengths shorter than 525

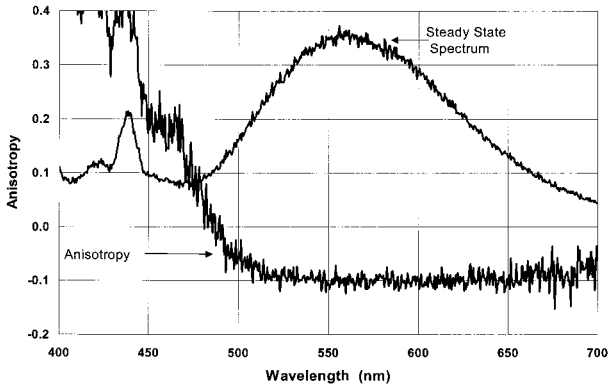

Figure 4. The steady state emission spectrum (arbitrarily scaled) and emission anisotropy from **1** excited at 388 nm in G1000 silicon oil at −12 °C. Note, both plots use the same zero along the *y*-axis. The emission at wavelengths shorter than 525 nm is contaminated by traces of a donor-only impurity.

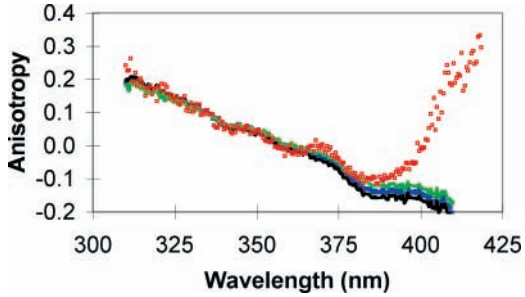

Figure 5. Excitation anisotropy profile for **1** detected at 600 nm in G1000 silicon oil at −11 °C. Experimental data (□), $Q_y = -0.035$ (black line), $Q_y = 0.00$ (blue line), $Q_y = 0.04$ (green line).

nm, trace donor fluorescence, and a solvent Raman peak contaminate the emission spectrum.[27] The negative sign and wavelength independence of the emission anisotropy suggest that if the CT emission derives intensity by borrowing oscillator strength from anthracene (donor) or ethylene (acceptor) transitions, the polarizations of all involved emission transition dipoles are very similar and are very different from the absorption polarization at 388 nm. The wavelength independence of the emission anisotropy indicates that one set of Q_ξ should suffice for all emission wavelengths between 525 and 700 nm.

The excitation wavelength dependence of the steady state emission anisotropy from **1** in G1000 at −11 °C (squares, Figure 5) is dramatically different from that of **2** (Figure 1). The polarization anisotropy from **1** *decreases* as the excitation wavelength is moved from 310 to 385 nm. There is a slight modulation, most notable as a peak at 370 nm and a shoulder at 350 nm. Above 390 nm, the anisotropy increases sharply with increasing excitation wavelength, reaching values greater than 0.25 at $\lambda_E > 415$ nm. The change in slope and sign of the anisotropy for excitation wavelengths above 390 nm cannot be rationalized using the R_x and R_y determined from **2** (vide infra). This portion of **1**'s absorption spectrum must contain an optical transition not present in **2**. The transition dipole direction for this transition is very similar to that of the CT emission and is reasonably assigned as an $S_0 \rightarrow$CT absorption band.[28] The CT absorption line shape will be determined after the Q_ξ of the CT→S_0 emission have been evaluated.

Values of Q_x, Q_y, and Q_z for the CT→S_0 emission in **1** are needed to evaluate $|V|_{S_1 \leftrightarrow CT}$. The transition dipole for the CT→S_0 emission is not constrained to lie in the plane of the anthracene. The acceptor is displaced (along the negative z direction, Chart 1) from the *xy* (anthracene) plane. A Mulliken type CT→S_0 transition will have a nonzero value of the fractional emission polarization along the *z*-axis, Q_z. Thus, the simplification used for **2**, $Q_x = 1 - Q_y$, is not valid for **1** and the full expression for Σ in eq 2 for must be used. Provided **1** is excited within the $S_0 \rightarrow S_1$ anthracene transition, $R_z = 0$ (vida supra) and the expression for Σ becomes a function of only two unknown quantities, Q_x and Q_y,

$$\Sigma = R_x(\lambda_{ex})Q_x(\lambda_M) + R_y(\lambda_{ex})Q_y(\lambda_M) \qquad (4)$$

As noted above, the anisotropy of the CT→S_0 transition is wavelength independent. A single value of Q_x and of Q_y is appropriate for the entire CT emission band. An analysis was performed using data from $\lambda_M = 600$ nm. The motion free FPA values for **1** were obtained from time resolved, polarized fluorescence decays collected in G10000 silicone oil at −12 °C, following excitation at 388 nm. The time-resolved anisotropy at 550, 575, and 600 nm decayed slightly during the CT state lifetime (< 1 ns). The motionless anisotropy was -0.115 ± 0.005, a value slightly more negative than from the steady state spectra.[29] To account for this difference, the steady state anisotropy data from **1** was multiplied by 1.09 prior to the following analyses.

The fractional absorption coefficients (R_x, R_y) from the dimethoxyanthracene chromophore in **2** can be used to determine the fractional components of the CT→S_0 emission, Q_ξ, *provided* the proximity of the acceptor to the anthracene in **1** does not substantially perturb the anthracene $S_0 \rightarrow S_1$ absorption spectrum and any contributions from the $S_0 \rightarrow$CT transition are very small. Both criteria appear to be satisfied in the region from 310 to 360 nm. Q_x and Q_y were treated as adjustable parameters in a nonlinear least-squares fit of r(310−360 nm, 600 nm) using eq 4 for Σ, $R_x(\lambda)$ and $R_y(\lambda)$ of the dimethoxyanthracene chromophore, and eq 2 for r.[30] An unconstrained regression analysis yielded $Q_x = 0.991$, $Q_y = -0.035$, and, by difference, $Q_z = 0.044$ (lower solid line, Figure 5). This indicates that the CT→S_0 emission is predominantly *x*-axis polarized. A negative value of Q_y is not possible. Additionally, these Q_x and Q_y values, combined with the R_x and R_y of the anthracene absorption, predict values of r(405−410 nm, 600 nm) that are more negative than −0.2 when substituted into eq 2.[31] A regression analysis performed with the constraint $Q_y \geq 0$ yielded $Q_x = 0.960$, $Q_y = 0.00$, and $Q_z = 0.040$ (middle solid line, Figure 5). The $r(\lambda, 600)$ profiles calculated using the constrained and nonconstrained (Q_x, Q_y) overlap the data and each other throughout the 310−360 nm region. At $\lambda_{ex} > 370$ nm, the anisotropy profile predicted with $Q_y = 0$ lies slightly above the $Q_y = -0.035$ prediction and yields $r = -0.19$ at 410 nm. To explore the influence of Q_y on fit quality, a regression value of Q_x was determined with Q_y fixed to 0.04. This yielded $Q_x = 0.918$, $Q_y = 0.040$, $Q_z = 0.042$ and a predicted anisotropy curve (upper solid line, Figure 5) that lies below most of the data points between 310 and 325 nm and above all the data points between 350 and 360 nm. If Q_y is greater than zero, 0.04 is a generous upper limit. For the two sets of polarized CT emission transition probabilities, (0.960, 0.000, 0.040) and (0.918, 0.040, 0.042), the "effective" CT transition dipoles lie at angles of (11.5°, 90.0°, 78.5°) and (16.6°, 78.5°, 78.2°), from the *x*, *y*, and *z* axes, respectively.

As noted above, the abrupt increase of the excitation anisotropy from **1** at wavelengths greater than 385 nm indicates the presence of a CT absorption band. Small differences in the absorption line shapes of different donor-only model compounds and of **1** complicated determination of the CT band shape by spectral subtraction.[32] At wavelengths where the $S_0 \rightarrow S_1$ and

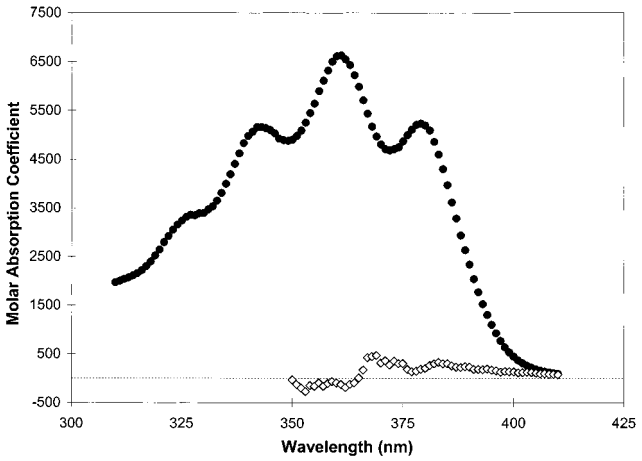

Figure 6. The CT absorption band of **1** (◇) determined from the total absorption spectrum (●) and the excitation polarization anisotropy profile at wavelengths greater than 350 nm. The dashed line corresponds to $\epsilon = 0$.

$S_0 \rightarrow$CT absorption bands overlap, the observed extinction coefficient is the sum of the extinction coefficients of the individual transitions, $\epsilon_{obs} = \epsilon_{CT} + \epsilon_{S1}$.
[33] The observed polarized
absorption components are weighted averages of those from the individual transitions:

$$R_\xi = \left(\frac{\epsilon_{CT}}{\epsilon_{obs}}\right) R_\xi^{CT} + \left(1 - \frac{\epsilon_{CT}}{\epsilon_{obs}}\right) R_\xi^{S_1} \quad (5)$$

Substitution of eq 5 into eq 2 yields the following expression for $\epsilon_{CT}/\epsilon_{obs}$. All quantities in eq 6 are known with the exception of R_ξ^{CT}.

$$\frac{\epsilon_{CT}}{\epsilon_{obs}} = \frac{\dfrac{5r+1}{3} - \sum_{\xi=x,y,z} (Q_\xi^{CT} \times R_\xi^{S_1})}{\sum_{\xi=x,y,z} Q_\xi^{CT} \times (R_\xi^{CT} - R_\xi^{S_1})} \quad (6)$$

A simple approximation is to use the regression values of Q_ξ^{CT} in place of the $R_\xi^{CT}(\lambda)$. The Q_ξ^{CT} are the emissive analogue of the CT absorption polarizations and are wavelength independent. This approach yields a crude estimate of the CT absorption band (Figure 6). At wavelengths greater than 380 nm, the experimental anisotropy profile deviates significantly from the regression prediction (Figure 5). Use of eq 6 yields a maximum of the $S_0 \rightarrow$CT band at 383 nm with ϵ_{CT} equal to 330 M^{-1} cm^{-1}. The $S_0 \rightarrow$CT transition comprises 10% of the observed spectrum at 390 nm, 50% at 405 nm, and 75% at 410 nm. At wavelengths shorter than 380 nm, the analysis yields a second peak at 369 nm, with ϵ_{CT} equal to 470 M^{-1} cm^{-1} and a precipitous drop at shorter wavelengths. The experimental FPA (squares, Figure 5) exhibits a local maximum at 369 nm, which is the origin of this second maximum in the extracted $S_0 \rightarrow$CT spectrum. While this analysis establishes the presence of a weak $S_0 \rightarrow$CT absorption band, the data is insufficient to generate accurate values of the bandwidth or maximum.

C. Calculated Dipole Moments and Coupling Matrix Elements in 1. The dipole moments and transition dipole moments among the relevant singlet states of **1** were calculated using the ZINDO/CI method[34] (Table 1). The acceptor ester groups can rotate about the C−C single bond connecting the C═O and C═C moieties. To avoid enforcing a mirror plane symmetry element in the calculations, the structure was minimized (molecular mechanics) starting from a geometry in which one C═C−C═O unit had an *s*-cis conformation and the other was *s*-trans. The calculated anthracene $S_0 \leftrightarrow S_1$ transition dipole moment is displaced by 0.9° from the *y*-axis. The calculated $S_0 \leftrightarrow$CT transition dipole moment makes angles of 14.1°, 89.6°, and 75.9° with the *x*, *y*, and *z* axes, respectively, which yields polarized components of the CT emission (and absorption) of $Q_x = 0.941$, $Q_y = 0.0$, and $Q_z = 0.059$.[35]

TABLE 1: Cartesian Components[a] of the State and Transition Dipole Moments in 1

	S_0	S_1[b]	CT	$S_0 \leftrightarrow S_1$	$S_0 \leftrightarrow$CT
x	0.816 D	−3.331 D	32.118 D	0.087 D	0.556 D
y	2.519 D	2.419 D	2.856 D	5.484 D	0.004 D
z	3.484 D	3.387 D	11.335 D	0.008 D	0.140 D

[a] With the reference frame origin at the middle of the anthracene, the positive halves of the *x* and *z* axes extend away from the acceptor (Chart 1). (b) S_1 refers to the lowest energy, locally excited state of the anthracene chromophore.

Generalized Mulliken Hush calculations[36] were performed to determine the coupling between the diabatic S_0, S_1, and CT states. The energies, dipole moments, and transition dipole moments from the ZINDO/CI calculations were used as input. The calculated coupling matrix elements are $|V|_{S_0 \leftrightarrow CT} = 555$ cm^{-1} and $|V|_{S_1 \leftrightarrow CT} = 32$ cm^{-1}.

IV. Discussion

The anisotropy and polarization results for the 1,4-dimethoxyanthracene chromophore in **2** are consistent with results from structurally similar anthracene derivatives.[18,19] The origins of the absorption and fluorescence bands are polarized almost entirely along the *y*-axis ($R_y = 0.99 \pm 0.02$, $Q_y = 0.97 \pm 0.02$: 410 nm). As the excitation or emission wavelength is displaced from the origin, the *x*-axis (long-axis) components of the transitions increase (and the FPA decreases). Absorption in the 260−270 nm region is predominantly *x*-axis polarized. The anisotropy and polarization results for the CT$\rightarrow S_0$ emission from **1** differ markedly from those of the anthracene transitions in **2**. Specifically, the anisotropy of the CT$\rightarrow S_0$ emission in **1** (a) *decreases* as the excitation wavelength increases; from 0.2 at 310 nm to −0.1 at 385 nm, (b) *increases* sharply at excitation wavelengths longer than 385 nm, and (c) is independent of emission wavelength. Both the negative sign of the CT emission anisotropy (excited between 360 and 400 nm) and its negative slope versus excitation wavelength (310−385 nm) demonstrate that the CT$\rightarrow S_0$ emission is polarized in a direction orthogonal to the molecular *y*-axis. The sharp reversal of the anisotropy sign at wavelengths greater than 385 nm is due to a weak $S_0 \rightarrow$CT absorption band. The presence of this band prevented direct determination of the fractional *y*-polarization of the CT$\rightarrow S_0$ emission, Q_y, via excitation at wavelengths where $R_y \sim 1$ for the anthracene chromophore (Figure 2, $\lambda_{ex} > 400$ nm). As the alternative, an analysis of the anisotropy excitation profile from 310 to 360 nm yields $Q_y = 0$. The absence of *y*-polarized character in the emission demonstrates that electronic mixing of the CT and S_1 states in **1** is negligible. This result is expected for DBA molecules with rigorous mirror plane symmetry, because the CT and S_1 states have different electronic symmetries, A′ and A″, respectively. However, molecular mechanics calculations and crystal structures[37] of the acceptor indicate that the lowest energy structure incorporates a dissymmetric arrangement of the ester groups. This reduction of the molecular symmetry should increase the magnitude of $S_1 \leftrightarrow$CT mixing. It is also possible for the A′ CT state to mix with a″ vibrational

levels of the A″ S_1 state (overall vibronic symmetry A′). These vibronic levels of S_1 have reasonable oscillator strength to $(a'')^1$ vibrational levels of the ground state. Such mixing is reported to contribute to the reduction of *y*-axis polarized $S_1 \rightarrow S_0$ fluorescence from anthracene and its derivatives upon increasing the emission wavelength.[38] The wavelength independence of the CT→S_0 emission anisotropy from **1** suggests that such mixing is not significant. As shown above, the best fit of the anisotropy data (Figure 5) indicates insufficient $S_1 \leftrightarrow$CT mixing to produce detectable *y*-axis polarization in the CT→S_0 emission. From a practical point of view, the $S_1 \leftrightarrow$CT coupling in DBA **1** is too small to measure accurately from fluorescence polarization anisotropy data.

Although the best-fit results indicate that $S_1 \leftrightarrow$CT mixing is negligible, an **upper limit** for this coupling can be derived from the upper limit on Q_y (0.04, vide supra) following the method of Gould et al.[10] The radiative rate constant of the CT→S_0 transition,[39] 1.1×10^7 s^{-1}, is determined by the CT$\leftrightarrow S_0$ transition moment according to $k_{rad} = n[(n^2 + 2)/3]^2 \times 313.7 \times \tilde{\nu}_{av}^3 \times M_{CT}^2$, where the average emission frequency $\tilde{\nu}_{av}$ is 18.1 kK and n is the solvent refractive index.[10] This yields a CT$\leftrightarrow S_0$ transition dipole moment, $M_{CT} = 1.5$ D. The *y*-component[35] of the transition dipole moment, $M_{CT,y} = \sqrt{Q_y} \times M_{CT}$, amounts to $\sqrt{0.04} \times 1.5$ D or 0.3 D. If one assumes that the entire y-polarized component of the CT→S_0 radiative rate constant arises from oscillator strength borrowed from the $S_1 \rightarrow S_0$ transition,[40] then the coefficient of the diabatic S_1 state in the adiabatic CT state can be estimated[10] as $C_{S_1} = M_{CT,y} / M_{D^*}$, where M_{D^*} is the transition dipole moment (*y*-polarized) of the anthracene $S_1 \rightarrow S_0$ transition. With $M_{D^*} = 3.32$ D,[41] C_{S_1} amounts to 0.09. The fraction of the diabatic anthracene S_1 state mixed into the adiabatic CT state is $\sim C_{S_1}^2$, which indicates that the diabatic S_1 state constitutes less than 1% of the adiabatic CT state.[42] By first-order perturbation theory, the $S_1 \leftrightarrow$CT electronic coupling may be related to the mixing coefficient and the energy gap between the states as

$$|V|_{S_1 \leftrightarrow CT} \approx (E_{S_1} - E_{CT}) \times C_{S_1} \approx (E_{S_1} - E_{CT}) \times M_{CT,y} / M_{D^*} \quad (7)$$

For eq 7, one requires the vertical energy gap between the S_1 and CT states at the CT state's equilibrium geometry. Thus, the energy denominator in the perturbation expression is calculated as the difference between the average emission energies, $\tilde{\nu}_{av}(D^*) - \tilde{\nu}_{av}(CT) = 3000$ cm^{-1}, instead of the free energy difference between the two states.[10] This establishes an upper limit on $|V|_{S_1 \leftrightarrow CT} = 3000$ $cm^{-1} \times 0.09 = 270$ cm^{-1}, which is substantial.[43] The preceding analysis is premised on a specific value of $Q_y = 0.04$. The relation between $|V|_{S_1 \leftrightarrow CT}$ and any value of Q_y can be demonstrated by substitution of $M_{CT,y} = \sqrt{Q_y} \times M_{CT}$ into eq 7, which yields $|V|_{S_1 \leftrightarrow CT} \approx 1360$ $cm^{-1} \times \sqrt{Q_y}$. Thus, if Q_y is greater than 0.006, the $S_1 \leftrightarrow$CT symmetry forbidden coupling across the 3-bond bridge is greater than 100 cm^{-1}. The upper limit of $|V|_{S_1 \leftrightarrow CT} \sim 270$ cm^{-1} (for $Q_y = 0.04$) is substantially larger than the value of 32 cm^{-1} derived from the GMH analysis of ZINDO transition moments and energies. Analysis of photoinduced charge separation rate constants in a 7-bond bridge analogue of **1** yielded 3 cm^{-1} for $|V|_{S_1 \leftrightarrow CT}$. Based on a diminution of the coupling per bond equal to 0.6 ($e^{-1/2\beta}$), one obtains a value of 23 cm^{-1} for $|V|_{S_1 \leftrightarrow CT}$ across the 3-bond bridge in **1**. This estimate and the GMH result predict that Q_y is between 10^{-4} and 10^{-3}, in good agreement with the best-fit analysis of the anisotropy data.

The $S_1 \rightarrow$CT electron-transfer rate in **1** is at least 3×10^{10} s^{-1}.[41b] How large must $|V|_{S_1 \leftrightarrow CT}$ be to achieve rates this fast? Comparison of spectroscopic energy gaps indicates $\Delta G°$ ($S_1 \rightarrow$CT) = −0.27 eV.[41b] The difference in energy of the S_1 and CT emission maxima yields 0.29 eV as an estimate of the total reorganization energy.[41b] This value is smaller than prior estimates of λ_V, 0.39 eV.[12] It is reasonable to assume that λ_S lies between 0.05 and 0.2 eV in the weakly dipolar siloxane polymers. Thus, to reproduce the above transfer rate constant using $\hbar\omega = 0.175$ eV and the above two λ_S values, $|V|_{S_1 \leftrightarrow CT}$ must be 39 and 48 cm^{-1}, respectively.[44] These values, which are within a factor of 2 of the GMH/ZINDO and seven-bond DBA derived estimates, predict $Q_y \leq 0.001$ for the CT emission, in accord with the best fit emission polarization results.

The GMH analysis predicts $|V|_{S_0 \leftrightarrow CT} = 550$ cm^{-1}. The ground and CT states have the same electronic symmetry and, in the dissymmetric conformation examined, their interaction is calculated to be 17 times larger than $|V|_{S_1 \leftrightarrow CT}$. The ZINDO/CI calculations predict the CT$\leftrightarrow S_0$ transition dipole moment is 0.57 D. This estimate of the transition moment is 2.6-fold smaller than the experimental value derived from the radiative rate constant, $M_{CT} = 1.5$ D. In addition to the direct, Mulliken contribution, $S_0 \leftrightarrow$CT oscillator strength could be borrowed from the energetically distant, but intense, 260 nm transition of the anthracene chromophore. As this $S_0 \leftrightarrow S_3$ transition is *x*-polarized; the *z*-polarized component of the observed CT transition moment can only arise from the direct $S_0 \leftrightarrow$CT transition. The *z*-polarized component may be estimated as $M_z(S_0 \leftrightarrow CT) = \sqrt{Q_z} \times M_{S_0 \leftrightarrow CT} = \sqrt{0.04} \times 1.5$ D = 0.30 D.[45] The GMH derived $S_0 \leftrightarrow$CT transition dipole moments predict the relative magnitudes of the *x* and *z* polarized components: $Q_x/Q_z = 0.941/0.059 = 16$.[45] This ratio can be used to estimate the *x*-component of the direct, Mulliken type transition dipole moment, $M_x(S_0 \leftrightarrow CT) = \sqrt{Q_x}/\sqrt{Q_z} \times M_z(S_0 \leftrightarrow CT) = \sqrt{16} \times 0.3$ D = 1.2 D, where the experimental value of $M_z(S_0 \leftrightarrow CT) = 0.30$ D is used. The total, Mulliken type contribution to the $S_0 \leftrightarrow$CT, transition dipole moment amounts to $\sqrt{(M_z(S_0 \leftrightarrow CT)^2) + (M_x(S_0 \leftrightarrow CT)^2)} = \sqrt{(1.2\text{ D})^2 + (0.3\text{ D})^2} = 1.25$ D. This is less than the experimental value of 1.5 D. If the CT→S_0 transition borrows *x*-polarized oscillator strength from the $S_0 \leftrightarrow S_3$ transition, the total transition dipole moment may be related to the Mulliken and borrowed transition moments as $\sqrt{[M_x(S_0 \leftrightarrow CT) + M_x(S_0 \leftrightarrow S_3)]^2 + M_z(S_0 \leftrightarrow CT)^2} = 1.5$ D. Presuming the *x*-polarized components of the direct $S_0 \leftrightarrow$CT transition moment and that borrowed from the $S_0 \leftrightarrow S_3$ transition have the same sign, the borrowed transition dipole moment amounts to $M_x(S_0 \leftrightarrow S_3) = 0.27$ D. The transition dipole moment of the band at 260 nm is ~10 D.[46] Following, the perturbation analysis described above, the coefficient of the S_3 diabatic state in the adiabatic CT state is 0.27 D/10 D or 0.027. The electronic coupling amounts to $|V|_{S_3 \leftrightarrow CT} = 0.027(E_{S_3} - E_{CT}) = 440$ cm^{-1}.[47] This symmetry-allowed $S_3 \leftrightarrow$CT coupling is comparable to the GMH estimate of the symmetry-allowed $S_0 \leftrightarrow$CT interaction.

V. Conclusion

The charge transfer state of **1** exhibits a weak ($\Phi = 0.02$) broad emission centered near 560 nm in nondipolar solvents. Analysis of the emission polarization anisotropy produced by $S_0 \rightarrow S_1$ excitation of the dimethoxyanthracene donor indicates that the emission's transition dipole moment lies within the approximate symmetry plane (*xz* plane) of the molecule. A perturbation analysis of the polarization data finds no measurable

coupling (<100 cm^{-1}) between the CT and S_1 states. Some coupling is necessary for the nonradiative $S_1 \rightarrow$CT transfer to occur. $|V|_{S_1 \leftrightarrow CT}$ estimates for **1**, derived from analysis of the $S_1 \rightarrow$CT transfer rate constant, from generalized Mulliken-Hush/ZINDO calculations, or by extrapolation from the coupling across a seven-bond bridge analogue of **1**, lie between 23 and 50 cm^{-1}, which is consistent with the absence of significant *y*-polarized (anthracene short-axis polarized) emission contributions. These estimates of the symmetry-forbidden $|V|_{S_1 \leftrightarrow CT}$ are 10−20 times smaller than the values determined for the symmetry-allowed $|V|_{S_0 \leftrightarrow CT}$ and $|V|_{S_3 \leftrightarrow CT}$ couplings in the same molecule. These results are in good agreement with prior investigations.[12] Analysis of CT emission anisotropy data does not provide high precision estimates of $|V|_{S_1 \leftrightarrow CT}$ when the coupling is small. Any coupling between S_1 and CT allows the CT$\rightarrow S_0$ transition to borrow oscillator strength from the $S_1 \rightarrow S_0$ transition. As the latter transition is *y*-polarized, $|V|_{S_1 \leftrightarrow CT}$ may be derived from Q_y, the fraction of the CT$\rightarrow S_0$ radiative rate constant that is *y*-polarized. For $Q_y = 0.02 \pm 0.02$, the coupling spans the wide range from 0 to 270 cm^{-1}.

Approximately four percent of the CT$\rightarrow S_0$ radiative rate constant arises from a transition dipole that is orthogonal to the anthracene plane (*z*-polarized). A direct, Mulliken type charge transfer transition is the most reasonable source of this contribution. The ratio of *x*-axis (anthracene long-axis) polarized and *z*-axis polarized transition dipole moments for the direct Mulliken type transition was determined using the generalized Mulliken-Hush method. The experimental *x*-axis polarized contribution is 0.27 D larger than the *x*-axis component of the direct Mulliken transition (1.2 D). Oscillator strength borrowed by mixing of the same symmetry S_3 and CT states, is proposed as the origin of this additional *x*-axis transition dipole contribution. The diabatic S_3 state constitutes 0.1% of the adiabatic CT state. The coupling between the two diabatic states, $|V|_{S_3 \leftrightarrow CT} = 440$ cm^{-1}, is similar to the ZINDO/GMH estimate of the coupling between the same symmetry S_0 and CT diabatic states, $|V|_{S_0 \leftrightarrow CT} = 550$ cm^{-1}.

The polarizations of the CT$\rightarrow S_0$ emission and of the anthracene $S_0 \rightarrow S_1$ transition, at its origin, are orthogonal. The emission anisotropy studies of **1** indicate the presence of a weak absorption, on the red edge of the $S_0 \rightarrow S_1$ band, with polarization characteristics that are similar (parallel) to that of the CT emission. This weak transition is assigned as a direct CT absorption band. While CT absorption bands have been identified in related molecules, the transition in **1** is not detectable by comparisons of absorption spectra from DBA and DB molecules.[48] Finally, the reduced absorption spectra and fractional *x*- and *y*-axis polarized absorption and emission transitions were determined as a function of wavelength for the 1,4-dimethoxyanthracene chromophore in **2**. Both the absorption and emission bands are almost entirely *y*-axis polarized at the S_0-S_1 origin. The fractional *x*-axis polarization of the absorption increases as the excitation wavelength is reduced. The fractional *x*-axis polarization of the fluorescence increases as the emission wavelength is increased. These variations in polarization with wavelength are in qualitative agreement with the characteristics of anthracene and structurally related derivatives.

Acknowledgment. Financial support from the National Science Foundation (grants CHE-9708351 and CHE-0108945) is gratefully acknowledged.

Supporting Information Available: Figure S1, the steady state, wavelength-dependent anisotropy curves predicted from experimental results. This material is available free of charge via the Internet at http://pubs.acs.org.

References and Notes

(1) (a) Kestner, N. R.; Logan, J.; Jortner, J. *J. Phys. Chem*. **1974**, *78*, 2184. (b) Bixon, M.; Jortner, *J. Chem. Soc., Faraday Discuss.* **1982**, *74*, 17.

(2) (a) Helms, A.; Heiler, D.; McLendon, G. *J. Am. Chem. Soc*. **1991**, *113*, 4325. (b) Oevering, H.; Paddon-Row, M. N.; Heppener, M.; Oliver, A. M.; Cotsaris, E.; Verhoeven, J. W.; Hush, N. S. *J. Am. Chem. Soc*. **1987**, 109, 3258. (c) Winkler, J. R.; Gray, H. B. *J. Biol. Inorg. Chem*. **1997**, *2*, 399.

(3) (a) Closs, G. L.; Calcaterra, L. T.; Geen, N. J. Penfield, K. W.; Miller, J. R. *J. Phys. Chem*. **1986**, *90*, 3673. (b) Gould, I. R.; Young, R. H.; Moody, R. E.; Farid, S. *J. Phys. Chem*. **1991**, *95*, 2068.

(4) (a) Marcus, R. A. *J. Phys. Chem*. **1989**, *93*, 3078. The radiative rate constant depends on the average emission frequency, which is determined by the driving force and reorganization energy.

(5) Mulliken, R. S. *J. Am. Chem. Soc*. **1952**, *74*, 811.

(6) Creutz, C.; Newton, M. D. Sutin, N. *J. Photochem. Photobiol. A* **1994**, *82*, 47. It is not simple to establish the value of $\Delta\mu$ when $|V|$ is large.

(7) Murrell, J. N. *J. Am. Chem. Soc*. **1959**, *81*, 5037.

(8) Pasman, P.; Rob, F.; Verhoeven, J. W. *J. Am. Chem. Soc*. **1982**, *104*, 5127.

(9) While S_1 formally refers to the lowest energy singlet excited state in a molecule, in this manuscript the term S_1 refers to the lowest energy singlet state of the donor chromophore.

(10) Gould, I. R.; Young, R. H.; Mueller, L. J.; Albrecht, A. C.; Farid, S. *J. Am. Chem. Soc.* **1994**, *116*, 8188.

(11) Bixon, M.; Jortner, J.; Verhoeven, J. W. *J. Am. Chem. Soc.* **1994**, *116*, 7349.

(12) (a) Zeng, Y.; Zimmt, M. B. *J. Am. Chem. Soc*. **1991**, *113*, 5107. (b) Zeng, Y.; Zimmt, M. B. *J. Phys. Chem*. **1992**, *96*, 8395. (c) Kumar, K.; Kurnikov, I. V.; Beratan, D. N.; Waldeck, D. H.; Zimmt, M. B. *J. Phys. Chem. A* **1998**, *102*, 5529.

(13) The nature of S_1 in anthracene and its derivatives is discussed in refs 18−20.

(14) Oliver, A. M.; Paddon-Row, M. N.; Kroon, J.; Verhoeven, J. W. *Chem. Phys. Lett.* **1992**, *191*, 371.

(15) Yip, W. T.; Levy, D. H.; Kobetic, R.; Piotrowiak, P. *J. Phys. Chem. A* **1999**, *103*, 10.

(16) There is no detectable CT absorption or emission band in DBA **2** (or **3**).

(17) Lakowicz, J. R. *Principles of Fluorescence Spectroscopy*; Plenum Press: New York, 1983.

(18) Michl, J.; Thulstrup, E. W. *Spectroscopy with Polarized Light*; VCH Publishers: New York, 1986.

(19) Friedrich, D. M.; Mathies, R.; Albrecht, A. C. *J. Mol. Spectrosc.* **1974**, *51*, 166.

(20) Brotin, T.; Waluk, J.; Desvergne, J.-P.; Bouas-Laurent, H.; Michl, J. *Photochem. Photobiol.* **1992**, *55*, 335.

(21) See Chapter 8.3.7 in reference 18.

(22) The electronic coupling between the donor and acceptor groups in molecule **2** is large enough to effect nanosecond transfer rate constants but too small to generate detectable charge transfer absorption or emission bands. Thus, the polarization of the anthracene absorption bands in **2** should be a reasonable model for those in **1**.

(23) Christensen, R. L.; Drake, R. C.; Phillips, D. *J. Phys. Chem*. **1986**, *90*, 5960.

(24) The *y*-axis in the present manuscript corresponds to the *z*-axis in ref 20.

(25) At the concentrations employed (<50 μM), the optical density at 410 is less than 0.01. Excitation at 410 nm under these conditions yields an emission spectrum that is distorted by scattered light between 410 and 425 nm and by Raman scattering beyond 455 nm. Thus, the initial analysis of $r(410, \lambda)$ was limited to the 430−450 nm region.

(26) Friedrich et al. identify the first vibrational band in the *x*-polarized spectrum of anthracene as a false origin arising due to vibronic intensity borrowing from the B_b state.[19] Brotin et al. conclude that the *x*-polarized spectrum, starting within the third vibrational feature (27.5 kK) of 1,4-didecyloxyanthracene, arises from an L_b absorption.[20]

(27) Time-resolved fluorescence decays form DBA **1** at 420 nm, the maximum of the donor emission, contain a component ($>$ 50% of the amplitude) that follows the impulse response and a component (amplitude $<$ 50%) that decays with a lifetime similar to that of donor-only compound. The former component is, likely, residual fluorescence from S_1 prior to formation of the CT state. The latter component appears to be a trace amount of donor-only impurity.

(28) Oevering, H.; Verhoeven, J. W.; Paddon-Row, M. N.; Warman, J. M. *Tetrahedron* **1989**, *45*, 4751.

(29) Upon excitation of **1** at 386 nm in a 155 K methylcyclohexane glass, the CT emission anisotropy is -0.12 ± 0.01, in agreement with the motionless anisotropy. Fidler, V.; Kapusta, P., private communication.

(30) The curve was fit between 310 and 360 nm to minimize the influence of the CT absorption band. The least-squares analysis was performed using the Solver routine within Excel 7.0.

(31) This prediction is for excitation of an $S_0 \rightarrow S_1$ transition without interference from a CT absorption band.

(32) The molecule formed by reduction of the alkene group in the acceptor of **1** should be a reasonable model for determination of the CT band shape by difference measurements. However, the vibrational features in the absorption spectrum of this compound are broadened and shifted by 1−2 nm relative to **1** and, surprisingly, to **2** as well. Use of different donor-only molecules to determine the CT absorption line shape, by difference, produces inconsistent results.

(33) Because the two transitions result in different final electronic states, it is valid to add the extinction coefficients (as opposed to the transition moments).

(34) Zerner, Michael C. In "Problem Solving in Computational Molecular Science", *NATO ASI Ser., Ser. C* **1997**, *500*, 249−289. The CI calculation proceeded from a closed shell reference using a single reference determinant and included all singly excited configurations formed by promoting an electron in the HOMO to the 100 lowest energy, vacant orbitals.

(35) The *x*-component of the CT state radiative rate constant, k_x^F, is proportional to the square of the *x*-component of the transition dipole moment, μ_x^{TR}. $Q_x = k_x^F/(k_x^F + k_y^F + k_z^F)$. Thus, Q_x may be equated to the squared cosine of the angle between the transition dipole moment and the *x*-axis or, equivalently, to $(\mu_x^{TR})^2/[(\mu_x^{TR})^2 + (\mu_y^{TR})^2 + (\mu_z^{TR})^2]$.

(36) (a) Cave, R. J.; Newton, M. D. *Chem. Phys. Lett.* **1996**, *249*, 15. (b) Cave, R. J.; Newton, M. D. *J. Chem. Phys.* **1997**, *106*, 9213.

(37) Sass, R. L.; Ratner, L. *Acta Crystallogr.* **1963**, *16*, 433.

(38) Sackmann, E.; Möhwald, H.; *J. Chem. Phys.* **1973**, *58*, 5407.

(39) (a) The CT state emission quantum yield, lifetime, and radiative rate constant in methylcyclohexane are 0.019, 1.8 ns, and 1.1×10^7 s^{-1}, respectively.[39b] The refractive index is 1.42. The average emission frequency of the CT→S_0 band is calculated[10] as $\nu_{av} = \int(\nu^{-2} I_\lambda \, d\nu)/\int(\nu^{-3} I_\lambda \, d\nu)$. (b) Source: Han, H. Ph.D. Thesis, Brown University, Providence, RI, 1998.

(40) Optical transitions of the cyclobutenediester acceptor are also *y*-polarized. The moderate oscillator strength and high energy of these transitions makes them a poor source of oscillator strength for the CT→S_0 transition.

(41) (a) The compound used for this determination was obtained by hydrogenation of the alkene group in **1**. The fluorescence quantum yield, lifetime, radiative rate constant and average emission energy of its $S_1 \rightarrow S_0$ transition in nondegassed methylcyclohexane are 0.65, 7.9 ns, 8.2×10^7 s^{-1}, and 21.1 kK, respectively.[41b] The radiative rate constant is equal to $n \times [(n^2 + 2)/3]^2 \times 313.7 \, \tilde{\nu}_{av}^3 M_{D^*}^2$ with ν_{av} calcualted[10] as $[(\int \nu^{-2} I_\lambda \, d\nu)/(\int \nu^{-5} I_\lambda \, d\nu)]^{-3}$. (b) Source: Morais, J. Ph.D. Thesis, Brown University, Providence, RI, 1995.

(42) The $S_0 \leftrightarrow S_1$ transition dipole moment calculated using the ZINDO/CI method is 60% larger than the experimental value. The latter was used to generate the upper limit estimate of $|V|(S_1 \leftrightarrow CT)$.

(43) (a) This analysis is valid in cases where the emitting state is overwhelming CT or LE. See eqs 20−24 in ref 10 for a more general analysis. (b) The difference in energy of the S_1 and CT emission maxima, after correcting for the intrinsic frequency dependence of the radiative process, is 3000 cm^{-1}.[39,41] (c) The difference in the equilibrium energies of the S_1 and CT states is 2200 cm^{-1}.[41b] Use of this energy gap yields estimates of $|V|_{S_1 \leftrightarrow CT}$ that are 30% smaller than those mentioned in the text.

(44) These values of $|V|$ were derived from the estimated rate constant using the semiclassical formulation of electron-transfer rate constant introduced in ref 1.

(45) The experimental transition dipole moment and that predicted by the ZINDO/CI calculation differ significantly. The relative values of the calculated *x* and *z* components will be used to factor the observed $M(S_0 \leftrightarrow CT)$ moment into direct (Mulliken) and borrowed contributions.

(46) (a) The integrated intensity of the 260 nm band in dimethoxyanthracene is ∼12-fold larger than that of the 380 nm band. Experimental and calculated ratios of these two bands' oscillator strengths in anthracene are 15−16:1.[46b] Thus, the transition dipole moment ratio for these bands is about 3−4:1. (b) Michl, J.; Thulstrup, E. W.; Eggers, J. H. *Ber. Bunsen-Ges. Phys. Chem.* **1974**, *78*, 575.

(47) The vertical energy gap from CT to the S_3 state is not known. The difference between the equilibrium S_1 state and CT state energies is 2200 cm^{-1}. Assuming that distortions of the S_1 and S_3 states to the CT equilibrium geometry incur the same energy increase, the vertical energy gap from the equilibrated CT state (22 300 cm^{-1}) to S_3 may be calculated as 36 400 cm^{-1} (the $S_0 \rightarrow S_3$ transition S_1 band energy) + 2200 cm^{-1} − 22 300 cm^{-1} = 16 300 cm^{-1}.

(48) (a) The $S_0 \leftrightarrow$CT transition moment may be estimated from the oscillator strength of the $S_0 \rightarrow$CT absorption band.[48b] For a Gaussian line shape, $M(S_0 \leftrightarrow CT) = \sqrt{(\epsilon_{max}/102)(\nu_{fwhm}/\nu_{max})}$, where ϵ_{max} is the extinction coefficient at the band maximum (M^{-1} cm^{-1}), ν_{fwhm} is the full width at half-maximum of the band, ν_{max} is the energy of the emission maximum, and $M(S_0 \leftrightarrow CT)$ is in units of Debye. Using $\epsilon_{max} \sim 400$ M^{-1} cm^{-1}, $\nu_{fwhm} \sim 3500$ cm^{-1}, and $\nu_{max} = 26\,000$ cm^{-1} (Figure 6) yields a transition dipole moment of 0.73 D. This value is 30% larger than the ZNDO/CI estimate (Table 1) and 50% smaller than the value derived from the CT→S_0 radiative rate constant. The 2-fold difference of the transition dipole moments derived from the CT absorption and CT emission analyses is significant. This difference may derive from (i) Q_ξ^{CT} not being a reasonable model for R_ξ^{CT} in eq 6, (ii) errors in quantum yield and radiative rate determinations for **1**, (iii) nonnegligible contributions of the $S_0 \rightarrow$CT absorption band in the 310−360 nm region used to determine Q_x^{CT} and Q_z^{CT} for the CT→S_0 transition, and (iv) structural differences in the equilibrium geometries of the S_0 and CT states that alter the transition dipole moments. The responsible combination of factors is not known. (b) Hush, N. S. *Coord. Chem. Rev.* **1985**, *64* 135.